Effect of Rust and Scale on the Bond Characteristics of Deformed Reinforcing Bars

By E. L. KEMP, F. S. BREZNY,

and J. A. UNTERSPAN

An experimental program was established to provide needed information on bond characteristics of ASTM A 432 bars with a broad range of scale and rust conditions. The principle parameter in the test series was the bar surface conditions.

It was concluded that the bond characteristics of deformed reinforcing bars with deformations meeting ASTM A 305 specifications do not appear to be adversely affected by varying degrees or types of surface rust or ordinary mill scale provided the weight of the bar meets the minimum ASTM weight and deformation height requirements. The deformation dimensions appear to govern bond characteristics of rusty bars, in that these bars exhibit a behavior similar to companion "as rolled" bars. The test data indicate that the current bond requirements are quite conservative, especially with regard to smaller bars because of the 800 psi (nom. 60 kgf/cm^2) maximum stress limit. Concrete strength appears to control the over-all bond behavior, particularly slip and deformation, to a much greater extent than the surface condition of the bar.

Keywords: bond (concrete to reinforcement); deformed reinforcement; reinforced concrete; reinforcing steel; research; rusting; scale (corrosion).

ACI member **E. L. Kemp** is professor and chairman, Department of Civil Engineering, West Virginia University, Morgantown, W. Va. Prior to joining West Virginia University he served with several consulting engineering firms in London, England, and as a fellow and instructor in the Department of Theoretical and Applied Mechanics, University of Illinois. Dr. Kemp studied at the University of Illinois where he received the BS and PhD degrees and at the Imperial College where he received the DIC and MSc degree. He is a chartered civil engineer in the United Kingdom. Currently, he is active on ACI Committees 115, Current Research, and 438, Torsion.

F. S. Brezny is a research assistant, Department of Civil Engineering, West Virginia University, Morgantown, W. Va. He received a BSCE degree from the same institution.

J. A. Unterspan is a Lieutenant, Army Corps of Engineers, Fort Benning, Ga. He was previously a research assistant in the Department of Civil Engineering, West Virginia University. He received a BS degree from the Citadel and an MSCE degree from West Virginia University.

■ SOME DIFFICULTY HAS BEEN encountered on construction sites recently with the rejection of reinforcing bars because of what has been judged to be excessive amounts of rust or mill scale. Such site rejections serve to emphasize the fact that current standards of acceptance are not precise in their definitions regarding allowable amounts of rust or mill scale. Although a considerable amount of research has been done on bond characteristics of mechanically clean deformed bars, little has been done on the effects of rust or mill scale on bond strength between concrete and deformed reinforcing bars meeting current ASTM specifications.

As the yield point of reinforcing bars is increased, higher bond forces must be developed if the bar capacity is to be fully utilized. Therefore, the influence of surface conditions on bond resistance has become increasingly important with the growing use of high strength bars. Previous research on this subject was largely confined to smooth or pre-A305 deformed bars. Only limited data were available for deformed bars conforming to A305 and apparently no information on higher strength A61, A432, and A431 deformed bars.* Thus, an experimental program was needed to investigate this matter.

*In the text A15, A16, A61, A305, A431, and A432 are ASTM specifications.

TABLE 1 — LEGEND USED FOR SPECIMEN NUMBERS (EXAMPLE X Y Z)

Letter X: Denotes series number where

A — indicates first series of tests with $f_c' \approx 3300$ psi

B — indicates second series of tests with $f_c' \approx 5600$ psi

Letter Y: Denotes bar size using ASTM Standard A305 bar number

Letter Z: Denotes surface conditions as described below:

A = Mechanically clean bars
B = "As Rolled" bars
C = Air rust—total exposure for 5½ months
C' = Air rust—total exposure for 3 months
D = Mechanically clean and lubricated bars
E = Heavy artificial scale condition
F = Intermediate artificial scale condition
G = Light mill scale condition
H = Fresh water rust for 5-1/2 months
I = Salt water rust for 5-1/2 months
J = Air rust - partial exposure for 5-1/2 months
K = Air rust - total exposure for 2 years
L = Fog room rust for 5-1/2 months

Note: A Roman numeral after the specimen number indicates either a change in concrete strength or specimen size for the same type of surface condition.

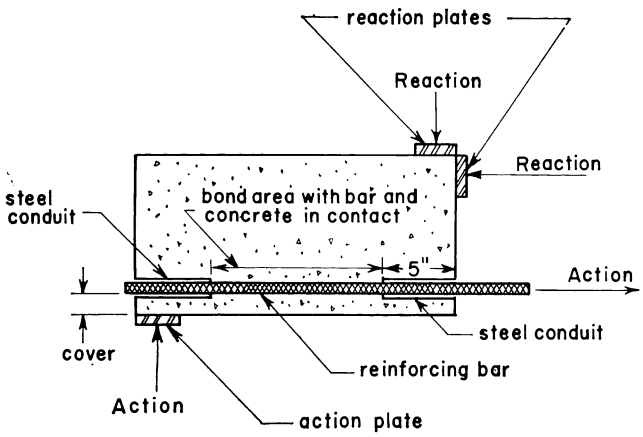

Fig. 1 — Schematic of cantilever bond test

OBJECT AND SCOPE OF RESEARCH PROGRAM

An experimental program was established to provide needed information on bond characteristics of A432 bars with a broad range of scale and rust conditions. The principal parameter in the test series was the bar surface condition (described in Table 1). Previous investigators noted a mode of failure change from simple bond pullout for smaller diameter bars to splitting action at bond breakdown for larger diameter bars (#7 and larger). Hence, tests were performed on #4 and #9 bars for each surface condition. A constant bond length was used for each bar size. Two companion series of specimens were cast with 3300 and 5600 psi (230 and 390 kgf/cm^2) concrete. Besides the main series of tests, a number of ancillary tests with other bar sizes and bond lengths were made; 159 specimens in all.

A new cantilever bond specimen was developed to overcome some objections raised regarding the standard ASTM pullout test. A schematic of such a specimen and test apparatus is shown in Fig. 1. Details and advantages of this improved test method are discussed herein.

PREVIOUS RELATED RESEARCH

The experimental evidence on the effects of surface rust on the bond characteristics of reinforcing bars is meager, although investigations date as early as 1909. Most of the investigations were based on smooth bars or bars not conforming to current ASTM deformation standards. Early work by Withey,[1] Abrams,[2] Shank,[3] and Gilkey, Chamberlin, and Beal[4] used smooth bars. Several surface conditions were studied by these investigators; rust, mill scale, sand blasted, and lubricated. The conclusion of these studies was that firm rust increased the bond resistance of smooth bars, since their bond resistance is largely dependent on surface adhesion between concrete and steel. For exposure periods up to 3 months, it was concluded that the bond developed by bars with undisturbed rust exceeded that for either unrusted or wiped rusted bars. After three months of rusting, smooth wiped bars proved superior to smooth undisturbed bars.

Probably the most extensive research on rusted deformed bars was by Johnston and Cox[5] in 1940, although the bars did not conform to ASTM A305. This investigation reported 420 bond pullout tests with 78 different bar sizes and degrees of rust. Results of the tests indicated that higher bond strengths were developed by rusted bars at low values of slip than by corresponding tests of unrusted bars. Furthermore, these investigators reported that the ultimate pullout strength of the bars was not greatly affected by their condition of rust. An attempt was also made to determine the bond pullout strength of wire brushed rusted bars. The results were inconclusive, in that increased bond strength resulted at low values of slip in some cases, whereas little effect was noted in other cases. Of greater significance, Johnston and Cox noted that the total amount of slip attained before reaching ultimate bond strength was greater for unrusted or slightly rusted bars than for heavily rusted bars.

The only prior study conducted on A305 deformed bars was in a similar series of bond tests reported by the Bureau of Reclamation[6] in 1956. It was concluded that rust is not harmful to bond between the concrete and steel and that there was no apparent advantage in removing any or all of the rust from the bars. Furthermore, it was noted that rust increased the steel surface's roughness and tended to augment the holding capacity of the bar.

SPECIMENS

All concrete for the specimens was made from locally available materials consisting of Type I portland cement, crushed limestone, and Ohio River sand. The following proportions and strengths were chosen for both series.

Series No.	f_c', psi (kgf/cm²)	Slump, in.(cm)	A/C	W/C	S/A	Wet curing, days	Test age, days
Series I	3300 (230)	3 (7.6)	7.0	0.6	0.4	none	16
Series II	5600 (390)	1 (2.5)	5.0	0.5	0.4	4	11

Reinforcing bars conformed to A432-64, whose deformation requirements are identical to A305-56T. To insure the greatest uniformity for the reinforcing bars, each size was supplied from a single heat of steel. The primary bar sizes for both series were # 4 and # 9, with ancillary tests using # 6, # 10, and # 11 bars (see Table 2). The stress-strain curves are shown in Fig. 2.

Use of the cantilever method of testing necessitated the development of a new type of bond specimen, a specimen based on ultimate strength criteria for both shear and flexure. In all but specimens with # 4 bars, shear was the controlling design factor. Since the shear at the point of bond breakdown could possibly approach the shear capacity of a plain section, inverted open stirrups were used so as not to restrain the main reinforcement and thus influence the bond resistance. In addition to design considerations for shear, the longitudinal reinforcement was kept at a sufficiently low percentage to avoid a concrete compression failure.

The embedment length L_e for each bar size was determined experimentally by pilot tests. Such lengths were chosen so that bar tensile stresses at the point of bond breakdown were between 45,000 and 60,000 psi (nom. 3200 and 4200 kgf/cm²). The embedment length for each size bar was made as long as practical, but not so long as to cause yielding of the bar before a bond failure occurred. The average bond strength was less, with greater embedment lengths, resulting in the most conservative comparisons of the different surface condition data with accepted code values. The embedment length for each bar size was held constant, re-

TABLE 2 — EXPERIMENTAL DATA FROM BOND TESTS

Specimen No.*	Bond stress, psi (kgf/cm²)			Bond stress ratio			f_c', psi (kgf/cm²)	Bulk of rust or scale specific gravity	Weight loss percent of theoretical weight
	0.01 in. (0.25 mm) slip, $u_{0.01}$	Bond breakdown u_{bb}	Ultimate u_u	$u_{0.01}/u_{ACI}$	u_{bb}/u_{ACI}	u_u/u_{ACI}			
B4A	1790 (125.8)	1800 (126.6)	1960 (137.8)	2.24	2.25	2.45	5300 (370)	—	—
B4B I†	1665 (117.1)	1800 (126.6)	2060 (144.8)	2.08	2.25	2.58	4800 (340)	2.57	0.67
B4B II†	1680 (118.1)	1770 (124.4)	2440 (171.5)	2.10	2.21	3.05	6100 (430)	2.57	0.67
B4C'	1760 (123.7)	1800 (126.6)	1985 (139.6)	2.20	2.25	2.48	6300 (440)	0.35	0.98
B4C	1650 (116.0)	1740 (122.3)	2000 (140.6)	2.06	2.18	2.50	5700 (400)	2.57	1.96
B4D	1320 (92.8)	1800 (126.6)	2015 (141.7)	1.65	2.25	2.52	5500 (390)	—	—
B4H	1420 (99.8)	1800 (126.6)	2440 (171.5)	1.78	2.25	3.05	5300 (370)	3.83	1.52
B4I	1560 (109.7)	1660 (116.7)	2440 (171.5)	1.95	2.08	3.05	5700 (400)	3.23	1.16
B4J	1630 (114.6)	1680 (118.1)	2000 (140.6)	2.04	2.10	2.50	6300 (440)	1.05	0.46
B4K	1630 (114.6)	1780 (125.1)	2005 (141.0)	2.04	2.23	2.51	5700 (400)	3.09	1.73
B4L	1800 (126.6)	1800 (126.6)	2485 (174.7)	2.25	2.25	3.11	6400 (450)	2.00	1.53
B9A	1030 (72.4)	1092 (76.8)	1225 (86.1)	1.60	1.69	1.90	5800 (410)	—	—
B9B I‡	748 (52.6)	1074 (75.5)	1123 (79.0)	1.20	1.74	1.81	5300 (370)	4.90	0.50
B9B	1028 (72.3)	1215 (85.4)	1333 (93.7)	1.63	1.94	2.11	5600 (390)	4.90	0.50
B9C'	1000 (70.3)	1100 (77.3)	1100 (77.3)	1.52	1.67	1.67	6000 (420)	6.24	0.67
B9C	950 (66.8)	1142 (80.3)	1347 (94.7)	1.43	1.72	2.03	6100 (430)	2.97	1.08
B9D	760 (53.4)	1142 (80.3)	1173 (82.5)	1.15	1.73	1.78	6100 (430)	—	—
B9H	930 (65.4)	1142 (80.3)	1298 (91.3)	1.48	1.82	2.06	5600 (390)	3.53	0.54
B9I	982 (69.0)	1172 (82.4)	1282 (90.1)	1.50	1.80	1.97	5900 (410)	4.03	0.90
B9J	1070 (75.2)	1120 (78.7)	1210 (85.1)	1.62	1.69	1.82	6100 (430)	2.52	0.64
B9K	960 (67.5)	1192 (83.8)	1285 (90.3)	1.46	1.81	1.95	6000 (420)	1.29	1.48
B9L	1050 (73.8)	1205 (84.7)	1335 (93.9)	1.58	1.81	2.01	6100 (430)	2.94	0.76
B6B	1050 (73.8)	1270 (89.3)	2028 (142.6)	1.31	1.59	2.42	6100 (430)	3.47	0.56
B6C	1285 (90.3)	1380 (97.0)	1871 (131.6)	1.61	1.73	2.34	5600 (390)	3.47	1.53
B10B	800 (56.2)	1230 (86.5)	1260 (88.6)	1.33	2.05	2.10	6200 (440)	8.00	0.24
B10C	820 (57.7)	1160 (81.6)	1160 (81.6)	1.36	1.93	1.93	6200 (440)	3.54	1.13
B11B	850 (59.8)	1020 (71.7)	1115 (78.4)	1.47	1.77	1.93	7000 (490)	10.00	0.41
B11C	682 (47.9)	1040 (73.1)	1110 (78.0)	1.20	1.83	1.96	6700 (470)	2.93	0.61
A4A	980 (68.9)	1440 (101.2)	—	1.23	1.80	—	3300 (230)	—	—
A4B	1230 (86.5)	1630 (114.6)	—	1.54	1.04	—	3300 (230)	2.67	0.28
A4C	1260 (88.6)	1600 (112.5)	—	1.57	2.00	—	3300 (230)	3.82	2.47
A4D	850 (59.8)	1590 (111.8)	—	1.06	1.99	—	3300 (230)	—	—
A4E	650 (45.7)	705 (49.6)	—	0.812	0.882	—	3300 (230)	5.52	27.40
A4F	800 (56.2)	815 (57.3)	—	1.00	1.04	—	3300 (230)	5.30	10.19
A4G	1040 (73.1)	1115 (78.4)	—	1.30	1.39	—	3300 (230)	5.15	7.05
A4H	1160 (81.6)	1390 (97.7)	—	1.45	1.74	—	3300 (230)	3.04	1.21
A4I	1230 (86.5)	1590 (111.8)	—	1.50	1.99	—	3300 (230)	2.80	1.39
A9A	750 (52.7)	850 (59.8)	—	1.55	1.75	—	3300 (230)	—	—
A9B	780 (54.8)	1000 (70.3)	—	1.61	2.06	—	3300 (230)	5.10	0.44
A9C	770 (54.1)	1000 (70.3)	—	1.59	2.06	—	3300 (230)	4.44	1.17
A9D	620 (43.6)	830 (58.4)	—	1.28	1.71	—	3300 (230)	—	—
A9E	580 (40.8)	752 (52.9)	—	1.20	1.55	—	3300 (230)	5.33	12.20
A9F	770 (54.1)	848 (59.6)	—	1.59	1.74	—	3300 (230)	5.41	4.83
A9G	860 (60.5)	860 (60.5)	—	1.77	1.77	—	3300 (230)	5.51	3.12
A9H	760 (53.4)	900 (63.3)	—	1.57	1.85	—	3300 (230)	4.10	0.57
A9I	680 (47.8)	885 (62.2)	—	1.40	1.82	—	3300 (230)	3.21	0.71
A9J	730 (51.3)	900 (63.3)	—	1.51	1.85	—	3300 (230)	4.16	0.51

*Refer to Table 1 for legend.

†Roman numeral indicates change in concrete strength.

‡Roman numeral indicates "A" series type specimen size used.

gardless of surface condition. Bond lengths, cover and other specimen details are presented in Table 3.

For each specimen, the ends of the test bar were inserted into steel conduits of slightly larger diameter. The conduit lengths were selected to leave the required embedment length exposed to concrete in the middle portion of the specimen, as shown in Fig. 1. The interior ends of these conduits were sealed with modeling clay to prevent the ingress of concrete mortar between the conduit and bar. By carefully following this procedure, a known bonding surface was assured for each specimen.

The previously mentioned artificial scale surface is unique in that the bars were heated for various periods of time at temperatures from 1500-1600 F (nom. 820-870 C) to produce a flaky scale that would be far worse than any normal mill scale. Both the surface appearance and the measured bulk specific gravities indicated that this artificial scale was excessive and would never occur in practice. The resulting surface was so delicate that special measures had to be taken to maintain the artificial scale during fabrication of the specimens. The bars used in the study are described in Table 1.

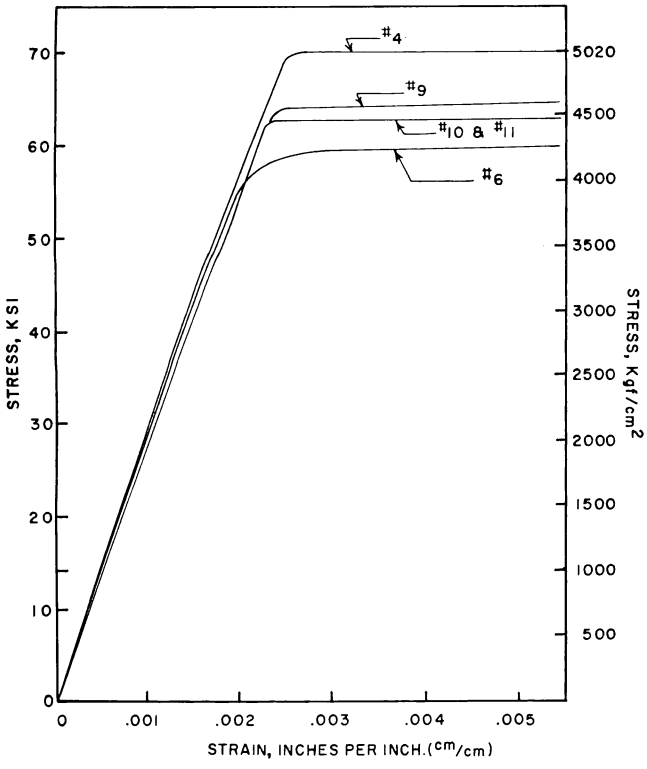

Fig 2 — Stress-strain curves for reinforcing bars

TEST APPARATUS

Several aspects of the cantilever bond test merit discussion. Such a test will produce bond stress situations similar to those existing along tensile reinforcing bars in flexural members. As opposed to the traditional pullout test, concrete and steel experience similar tensile strains and, in addition, cantilever test bond stresses are more representative of actual bond stresses in beams because both external shear and bending moment are present in the test specimen. Therefore, the cantilever beam test represents the bond situation existing between a flexural crack and the end of a simple beam and produces the same type of strain gradient. In many aspects, the cantilever test duplicates the behavior of the hammer-head beams tested by Watstein and Mathey[7] and the rectangular beams tested by Clark.[8,9] The cantilever test appears to be similar to these tests as well as the beam tests recommended by ACI 208-58 and ACI Committee 408,[10] but possesses the advantages of being smaller and cheaper. The relationships of bond, shear, and moment can be varied easily to produce different types of failures. The validity of this cantilever test with respect to the reported results of pullout and beam tests is discussed in the following sections.

The hydraulic loading system consisted of a pair of opposing couples, an action and a reaction separated by a known lever arm. The hydraulic ram loads were measured with load cells; the free-end and loaded-end slips were measured by mechanical dial gages (all as shown in Fig. 1). Load and slip measurements were taken at incremental load stages, stages that were carried either well beyond bond breakdown or until the bar yielded, thereby developing a complete load-slip curve for each specimen. Three specimens in both # 4 and # 9 bar sizes were prepared for each bar surface condition. Test results are tabulated in Table 2.

SPECIMEN BEHAVIOR

It is convenient to discuss the specimen behavior in two broad categories, namely those specimens with #9 bars or larger, and those with #6 bars and smaller.

Small bar specimens

Observations of the smaller bar specimens revealed a nearly linear relationship between load and slip up to approximately three-quarters of the ultimate bond stress, when the load-slip curve broke sharply; this is shown in Fig. 3 and 4. The curves after the breakdown of bond remained es-

TABLE 3 — DETAILS OF SPECIMENS

Specimen No.	Height, in. (cm)	Width, in. (cm)	Length, in. (cm)	Longitudinal steel moment reinforcement (other than test bar)		End reinforcement (closed rectangular stirrup) (each end)	Shear reinforcement (open U type stirrup)	Test bars embedment length, in. (cm)	Clear cover, in. (cm)
				Top	Bottom				
A4, B4	14 (35.6)	10.5 (26.7)	18 (45.7)	2 #3	2 #3	1 #2	None	5 (12.7)	1-3/4 (4.44)
A9, B6	14 (35.6)	14 (35.6)	28 (71.7)	2 #3	2 #3	1 #3	#3 @5-1/2 (14 cm)	A9-15 (38.1) B6- 8 (20.3)	1-7/16 (3.65)
B9	14 (35.6)	14 (35.6)	34 (86.4)	2 #3	2 #3 + 2 #4	1 #3	#3 @5-1/2 (14 cm)	15 (38.1)	1-7/16 (3.65)
B10	14 (35.6)	20 (50.8)	34 (86.4)	2 #4	2 #4	1 #3	#3 @5-1/2 (14 cm)	17 (43.2)	1-7/16 (3.65)
B11	14 (35.6)	20 (50.8)	40 (101.6)	2 #4	2 #4	1 #3	#3 @5-1/2 (14 cm)	19 (48.3)	1-7/16 (3.65)

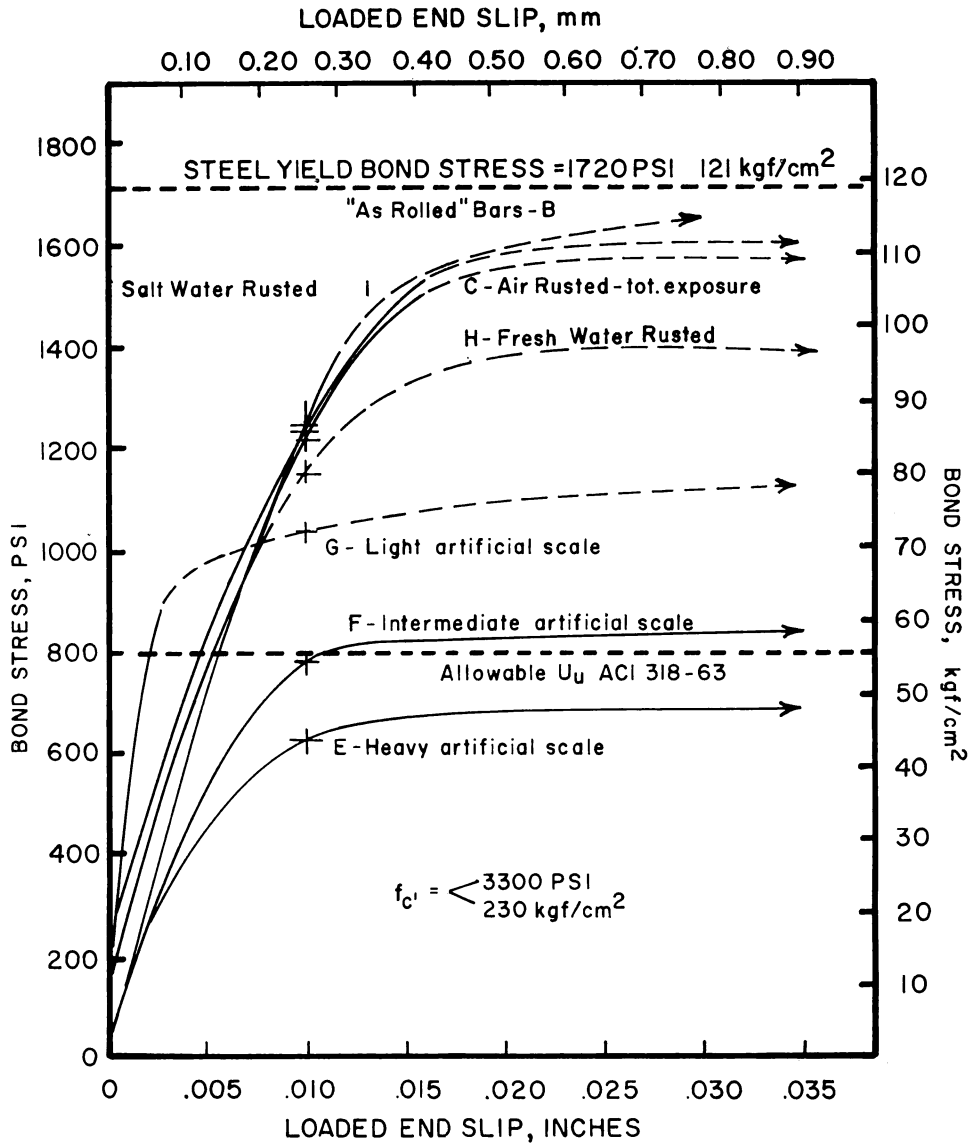

Fig. 3 — Family of # 4 bar curves (first series)

sentially horizontal, indicating increasing slip with little gain in bond resistance. This breakdown of bond occurred before the bars reached the yield point of the steel, as was intended by one of the parameters established for the tests. However, in every case except for bars with artificial scale, the bar yield point would have been reached before it pulled out of the specimen. All slip values were measured at the loaded end, for there was little evidence of free end slip even with only a 5 in. bond length.

The load-slip curves indicated that bar surface condition, for all but the artificial scale specimens, had little influence on the ultimate bond resistance compared to the other variables. Considerable loaded-end slip was measured at ultimate bond resistance indicating that most of the bond forces were developed through bearing of lugs against concrete. This would minimize the effect of surface conditions. Furthermore, despite the fact that the bond appears to be developed by bearing, there was no evidence of concrete splitting at failure for the smaller bar specimens.

The effect of surface condition on the initial slope of the bond-slip curve is more apparent in the second series, where surface rust was more widely varied. The as-rolled bars with normal mill scale had the least slip, followed in order by 2-year atmospheric rust, submerged-in-water rust, fog-room rust and, finally, a lubricated surface. The bars with atmospheric rust exhibited less slip than water-rusted bars which developed a more porous coating. Both the lubricated and heavy artificial scale surface conditions produced much more slip before ultimate was reached than any other specimens. However, concrete strength is a more significant variable than surface condition with regard to the slope of bond-slip curves. In the first series ($f_c' = 3300$ psi, 230 kgf/cm^2) bond breakdown in all but the artificial scale specimens occurred after a loaded end slip of 0.010 in., whereas in the second series ($f_c' = 5600$ psi,

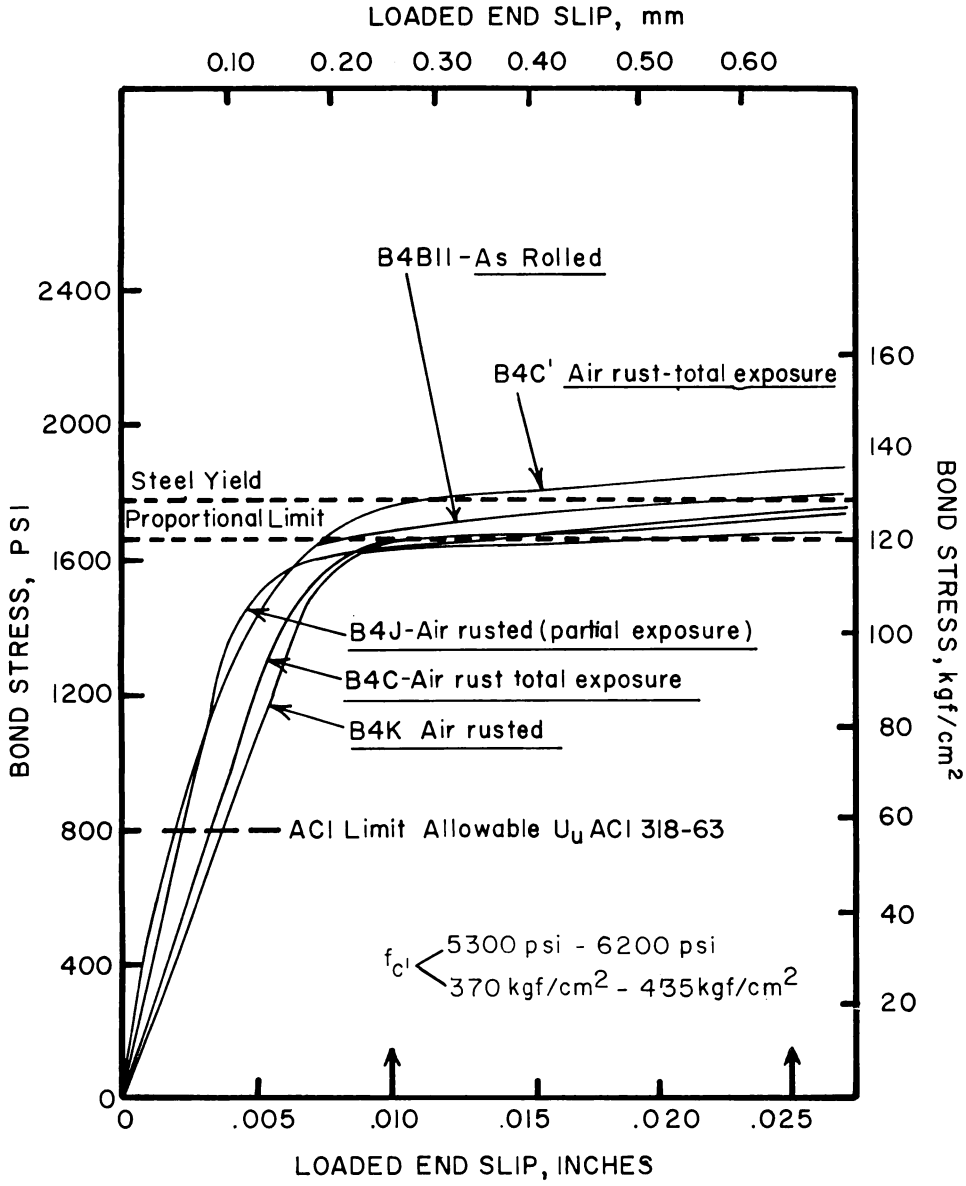

Fig. 4 — Family of # 4 bar curves (second series)

390 kgf/cm²) breakdown of bond occurred before a slip of 0.010 in. (0.25 mm).

The reported bond stresses were calculated from external loads on the bar and total surface area; representing an average value of stress along the bond length of the bar. Since internal bar strains were not measured, it was impossible to evaluate the local strain distribution or the maximum steel stresses along the bar. Nevertheless, failure commenced at the loaded end, progressively subjecting more of the bar to bond stresses to resist the increasing external force. A post-test examination of the bar and concrete surface revealed that high stress concentrations at the loaded end caused local disintegration of the concrete and attendant loss of bond. Thus, the portion of the bar resisting the external force increased as it progressed along the bar. Discounting the artificial scale cases, this shift was slight and did not involve the entire bond length even though this length was only five inches for the #4 bars. This was confirmed by the lack of any significant free end slip at any load stage.

Changing the bond length did not result in a change of bond-slip behavior, but instead influenced the average bond stress magnitude. This was expected, and is in agreement with prior research on bond development.

Large bar specimens

For the case of specimens using the larger #9, #10, and #11 bars, the initial behavior was quite similar to that of the smaller specimens. This can be seen by comparing the bond-slip curves, as shown Fig. 5 and 6. Thus, the conclusions reached regarding the influence of concrete strength and surface conditions also apply to larger specimens, although the specimen be-

havior changed dramatically as the loading increased and merits special mention.

The failure of larger specimens started in one of two ways. One involved the development of a longitudinal bond crack at the front face directly under the bar. This crack slowly propagated along the bar with increased loading and continued to where the conduit ended within the specimen. At this point, a flexural type crack formed perpendicular to the bond crack, but did not penetrate to the edge or up the side of the specimen. The other type of failure developed in the reverse order, in which a flexural crack formed across the specimen at the internal end of the conduit and was quickly followed by a longitudinal bond crack.

Regardless of the order of initial crack formation, the cracks widened and propagated in a similar manner. The bond crack lengthened with increasing load while one or more additional transverse cracks developed in the region of the bond length. Some of these transverse cracks progressed across the bottom of the specimen and advanced some distance up the side of the specimen. Observations revealed that the longitudinal bond crack preceded the development of the transverse cracks within the bond length. Thus, transverse cracks did not cause local bond slip but were associated with longitudinal bond cracks. At ultimate load the strain rate increased rapidly and the specimens failed by splitting of the concrete, resulting in a bar slip of from ¼ to 1 in. (nom. 6 to 25 mm). As the bond crack progressed toward the free end, a redistribution of stresses resulted since the bar force was no longer associated with the bending moment at a given point. In the specimens with large bars, the bond crack finally reached a point where the specimen could no longer redistribute the forces and the specimen failed in shear. Post-test photographs of the bottom and

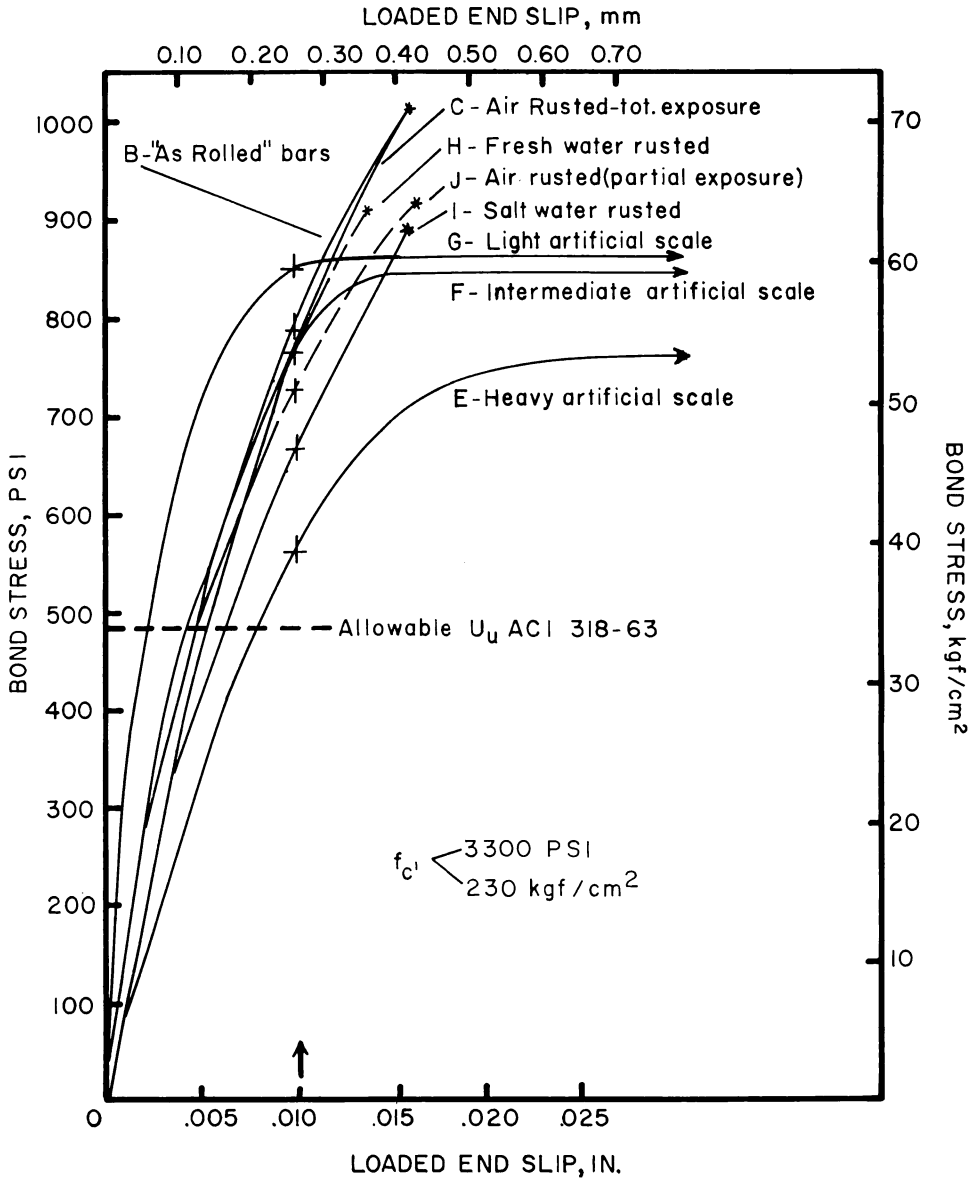

Fig. 5 — Family of # 9 bar curves (first series)

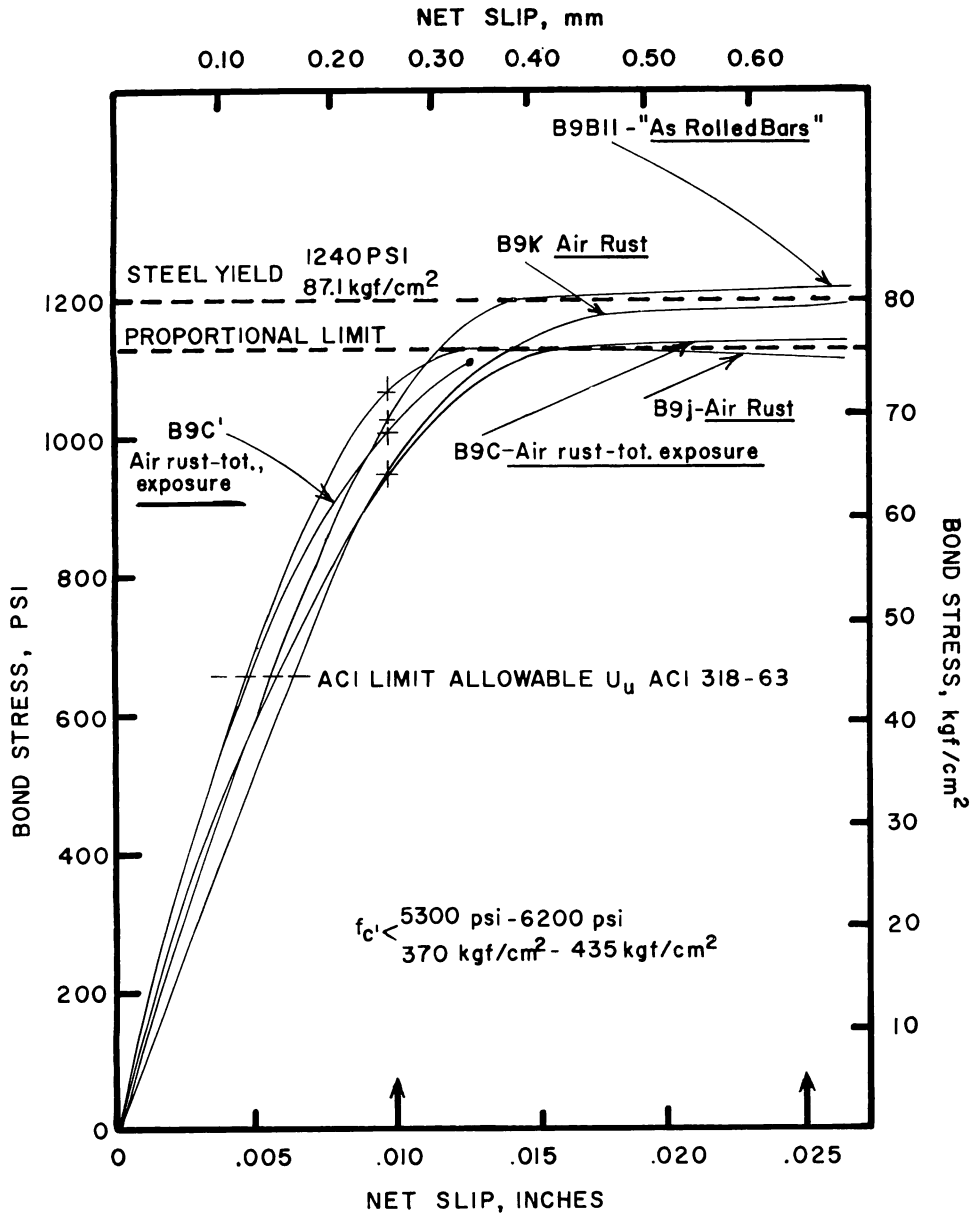

Fig. 6 — Family of # 9 bar curves (second series)

Fig. 7 — *Post-test* photograph of sides of typical # 9 specimens showing splitting failure

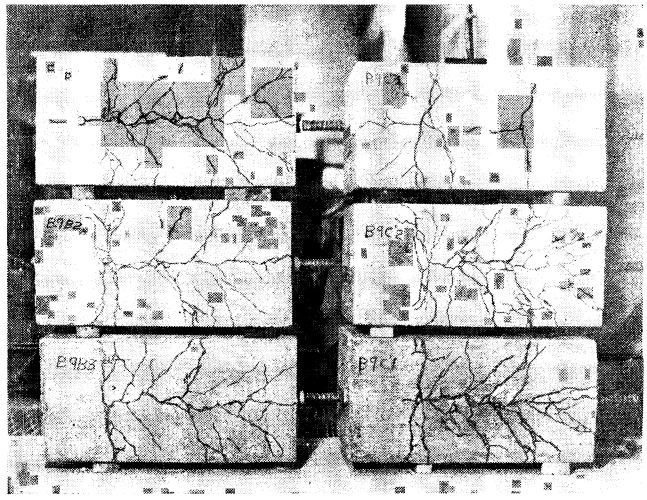

Fig. 8 — Post-test photograph of bottoms of typical # 9 specimens showing splitting failure

sides showing the splitting of typical #9 specimens are presented in Fig. 7 and 8.

TEST RESULTS

Ultimate bond stress

The bond-slip curves show that the average ultimate bond stress was little affected by the surface condition of the bars, except for the case of artificially scaled surfaces. For comparison of these test results with current ACI 318-63 code requirements[11] for ultimate bond stress:

$$U_u \leq \frac{9.5\sqrt{f_c'}}{D} \leq 800 \text{ psi}$$

bond stress versus weight loss curves are shown in Fig. 9. In this figure, bond stress was determined from the flattop portion of the bond-slip curves (after bond breakdown, but before either steel yielding or the attainment of ultimate bond stress). In most cases this stress was developed with a free-end slip of 0.025 in. (0.64 mm) or less; therefore, this stress represents a useful upper value which occurs before excessive cracking of the concrete.

The abscissa in Fig. 9 is the percentage weight ratio of the rust and/or scale to the theoretical bar weight based on the nominal bar diameter. This procedure was used to establish a site criterion for evaluating corroded bars. The weight of the corrosion product was obtained by comparing the weight of a corroded sample before cleaning to the weight of the sample after cleaning. The loss in steel weight would be less than the weight of rust because the corrosion product consists of hydrated iron oxide. On the basis of chemical analysis, it would be reasonable to assume that the loss of steel is between six-tenths and three-fourths of the percent ratio shown for rust and/or scale.

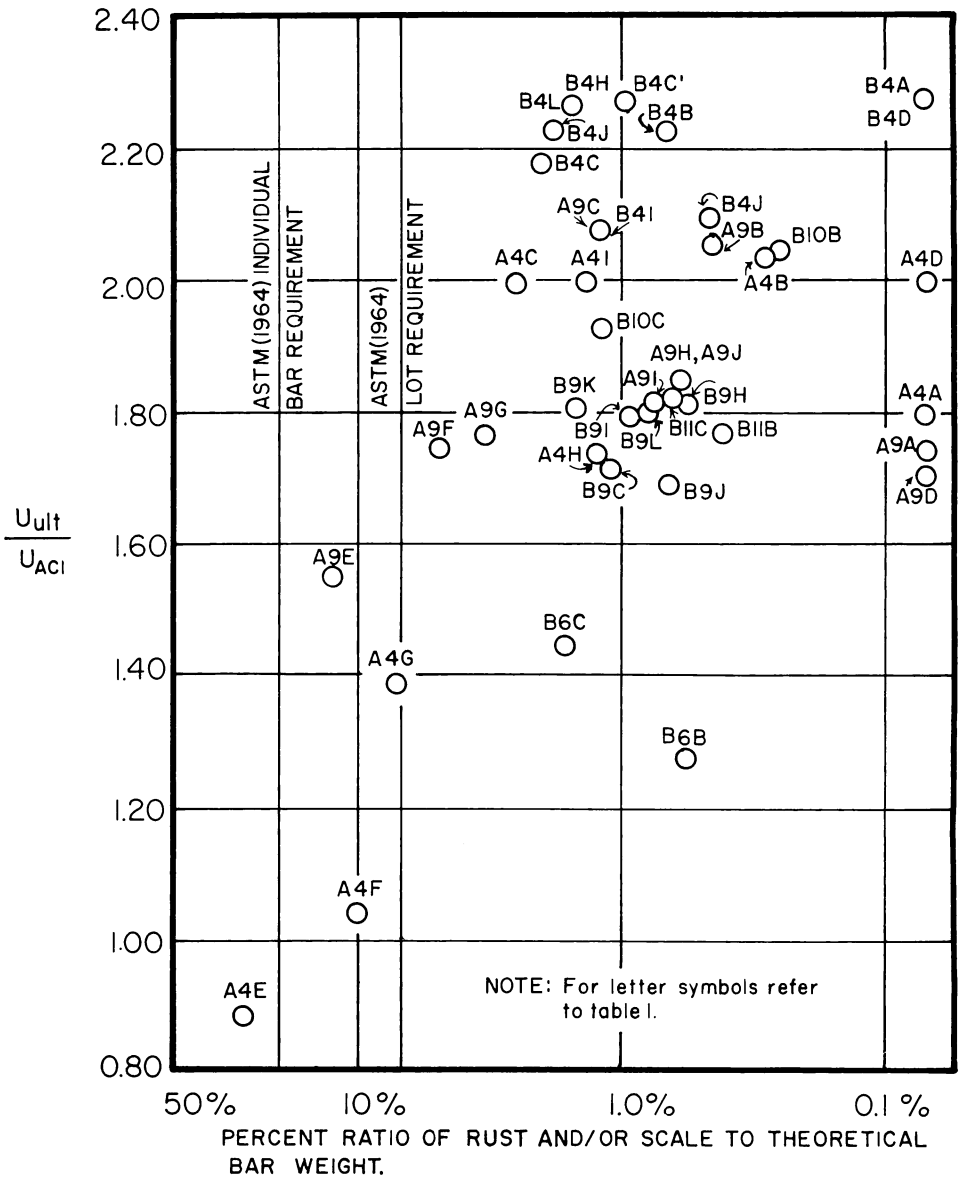

Fig. 9 — Effect of corrosion weight loss on the ultimate bond stress

Disregarding the artificial scale conditions, the remaining data show that the specimens developed average bond stresses at ultimate loads from 1.2 to 2.3 times the allowable ultimate stresses required by the ACI 318-63 Code. The bars with short-term air rust performed as well or better than "as rolled" bars although, in general, rusted bars exhibited a slight decrease in bond resistance. As the bar ages and more surface rust develops, the initial bond stress increases, followed by a slight decrease in bond stress as was previously observed by Gilkey, Chamberlin, and Beal.[4] It should be emphasized that the surface conditions of each bar were undisturbed during specimen preparation; a type of handling that would not be encountered in construction practices. Therefore, the data for rusted bars represent the worst possible case for a given surface condition.

Bond stress at 0.01 in. slip

It is also possible to define the useful ultimate stress U_c as that which occurs at a loaded end slip of 0.01 in. (0.25 mm). Although this slip value bears little relationship to bond strength, it may be viewed as a useful crack control criterion and has been so used by a number of investigators.[7,8,9] It would seem more appropriate to insure that this slip does not occur at service conditions, rather than use it as an ultimate bond requirement. Nevertheless, for its relationship to prior research, the results of using this stress as a failure criterion are shown in Fig. 10. The only significant difference between the curves of Fig. 9 and 10 is that the ratios of measured to allowable stress are lower and the data are more scattered. The lower ratios are to be expected since the 0.01 in. (0.25 mm) slip occurs for most of the low strength concrete specimens before the point of bond breakdown, and in this region the surface condition has much more influence than in the flat-top region. The test data are shown in Table 2.

Classification of corrosion

To distinguish the various types of surface corrosion and assess their amounts, the weight loss from bars, deformation heights and bulk specific gravity of corrosion products were determined. Although the oxides of iron have nearly the same density, the bulk specific gravities of test bars showed a considerable range. It was possible to distinguish several of the surface conditions on the basis of bulk specific gravity, especially the artificially scaled bars, but it was impossible to relate surface conditions or weight loss to bond performance. Bulk specific gravities varied from 2.7 to 4.5, while corresponding bond ratios varied from 1.2 to 2.3, as shown in Table 2. Deformation measurements are shown in Table 4. Note that the artificially scaled bars still meet the ASTM Standards for deformation height and spacing after the scale was removed.

Design criterion

From the various curves of bond stress versus slip, it is possible to develop a useful design criterion based on the flat-top ultimate bond stress illustrated in Fig. 9. Bars with rust and/or mill scale may be used and will be satisfactory with regard to bond resistance, provided that all cleaned samples meet the requirements specified by the ASTM relative to minimum height of deformations and permissible variation of theoretical weights, that is, that the permissible underweight of an individual bar shall not exceed 6 percent.

This criterion is influenced by initial weight, surface condition, and bond length of the bar. Considering surface conditions, all the specimens, other than those with artificial surfaces (scale, lubricated, cleaned) met the ACI ultimate bond strength criterion with a wide margin of safety. If a shipping lot of bars were overweight by the maximum permitted by the 1964 ASTM specifications, (3.5 percent) and then allowed to rust to such an extent that a representative cleaned sample was reduced to the minimum weight allowed, for an individual bar (6 percent underweight), then the steel loss would be about 9.5 percent, corresponding to a corrosion of between 14 and 16 percent. Even in such an extreme and unlikely case of corrosion, bond performance of the bars of the range of sizes used in the test series would still be satisfactory under current ACI 318-63 Code requirements. This statement is based on the extreme artificial scale specimens E, F, and G in Fig. 9, which represent a lower bound which would never be encountered in construction practice. In fact, 2-year air rust samples which had a thick coating of rust lost less than 5 percent weight upon cleaning. Unless deliberate action is taken to produce a special surface, it appears that bars would have to rust in water or air for extraordinarily long periods before a cleaned sample of a maximum overweight bar would be rejected on the basis of not passing a weight or deformation height test. In addition, it would be impossible to maintain these heavy coatings with normal handling on site, and any removal of this delicate surface would improve the bond resistance significantly.[4] None of the rusted samples had such heavy coatings, nor have any other investigators reported such cases; thus the necessity to use the artificial scale data to substantiate the bond criterion. Although bars larger than #11 were not tested it is reasonable to state that for any given environment causing rust, the thickness of rust would be about the same regardless of bar

TABLE 4 — SELECTED BAR DEFORMATION MEASUREMENTS

Specimen No.	Deformation height, in. (mm) Maximum	Minimum	Average	Minimum (ASTM)	Deformation spacing, in. (mm) Average	Maximum average (ASTM)
B4B	0.0403	0.0252	0.0318	0.020	0.248	0.350
	(10.23)	(6.40)	(8.08)	(5.1)	(62.9)	(88.9)
B6B	0.0535	0.0448	0.0489	0.038	0.386	0.525
	(13.59)	(11.38)	(12.42)	(9.7)	(98.0)	(133.4)
B9B	0.0903	0.0724	0.0828	0.056	0.526	0.790
	(22.94)	(18.39)	(21.03)	(14.2)	(133.6)	(200.6)
B10B	0.0983	0.0700	0.0798	0.064	0.598	0.889
	(24.97)	(17.78)	(20.27)	(16.3)	(151.9)	(225.8)
B11B	0.0919	0.0739	0.0817	0.071	0.669	0.987
	(23.34)	(18.77)	(20.75)	(18.0)	(169.9)	(250.7)
A4C*	0.0379	0.0301	0.0357	0.020	0.261	0.350
	(9.63)	(7.65)	(9.08)	(5.1)	(66.3)	(88.9)
A4E*	0.0360	0.0259	0.0318	0.020	0.260	0.350
	(9.14)	(6.58)	(8.08)	(5.1)	(66.0)	(88.9)
A9C*	0.0804	0.0682	0.0747	0.056	0.549	0.790
	(20.42)	(17.32)	(18.97)	(14.2)	(139.4)	(200.6)
A9E*	0.0879	0.0626	0.0766	0.056	0.545	0.790
	(22.33)	(15.90)	(19.45)	(14.2)	(138.4)	(200.6)

*Measured after cleaning the bar.

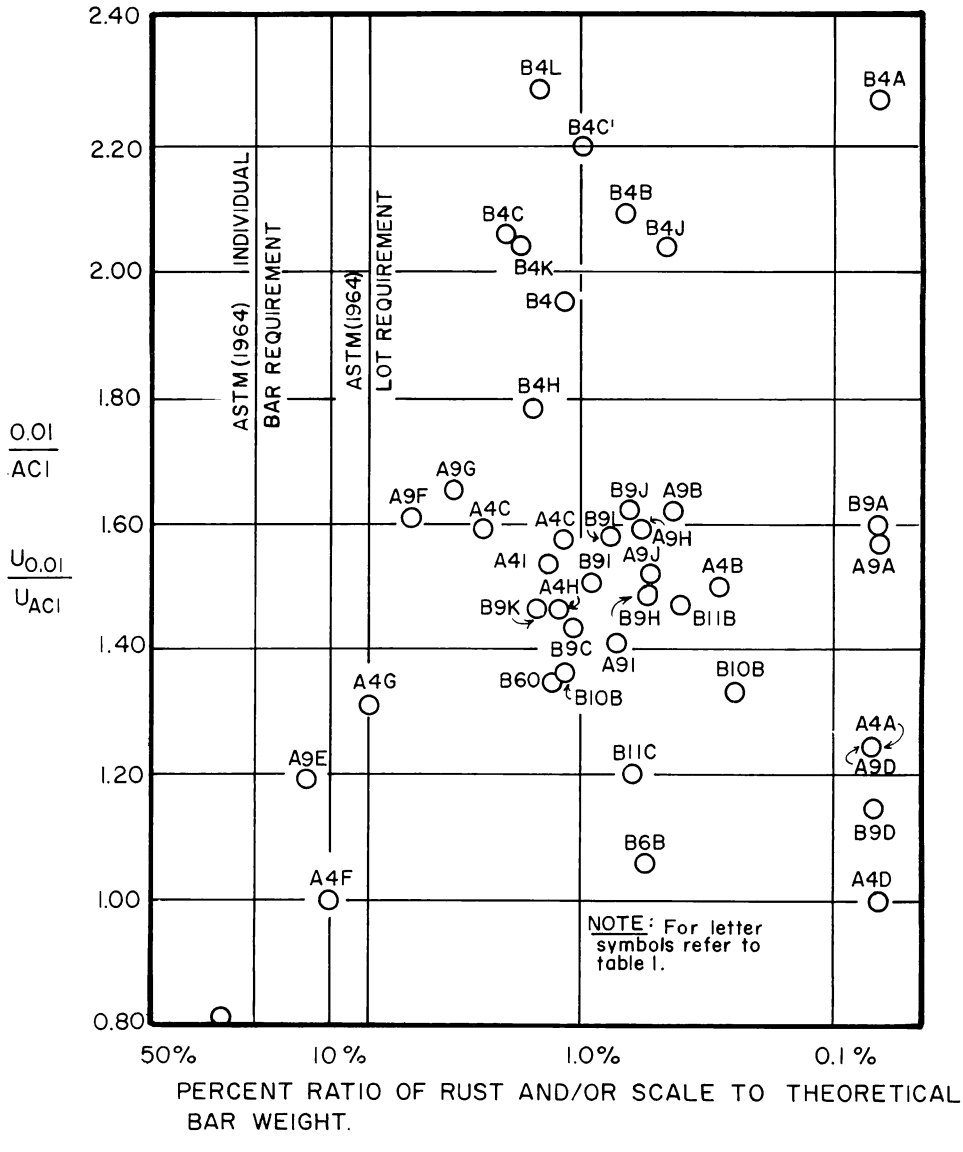

Fig. 10 — Effect of corrosion loss on the bond stress at 0.01 in. slip

size. Therefore, the bond performance relative to rust of larger diameter bars, which have higher deformations, should be superior to that of the bars tested.

Influence of bond length

As mentioned previously, bond length directly affects average bond stress because the entire exposed surface is used to compute the stress. Longer bond lengths in the case of smaller bars would have yielded the bar before the ultimate bond stress was obtained, whereas shorter lengths would have resulted in higher average bond stresses before failure. Even the larger bar specimens which failed by splitting did not show any measurable free end slip before failure. Therefore, the bond lengths used were longer than the actual length involved in resisting the bar force, resulting in average stresses which were lower than actual stresses. From this reasoning, the criterion based on computed average bond stresses is conservative.

Comparison of test data with current bond requirements

Since the various surface conditions did not affect the ultimate bond stress significantly, the entire body of data can be compared to the current ACI 318-63 bond requirements by plotting measured bond stress against $\sqrt{f_c'}/D$. In Fig. 11 bond stress for the solid points was determined from the flat top portion of the bond-slip curves described above. For the bars tested, it can be seen that the current requirement for the #9, #10, and #11 bars is conservative and does not even represent a lower bound to the data. In the case of the smaller bars, the 800 psi (56.2 kgf/cm^2) bond limit is unduly conservative and represents

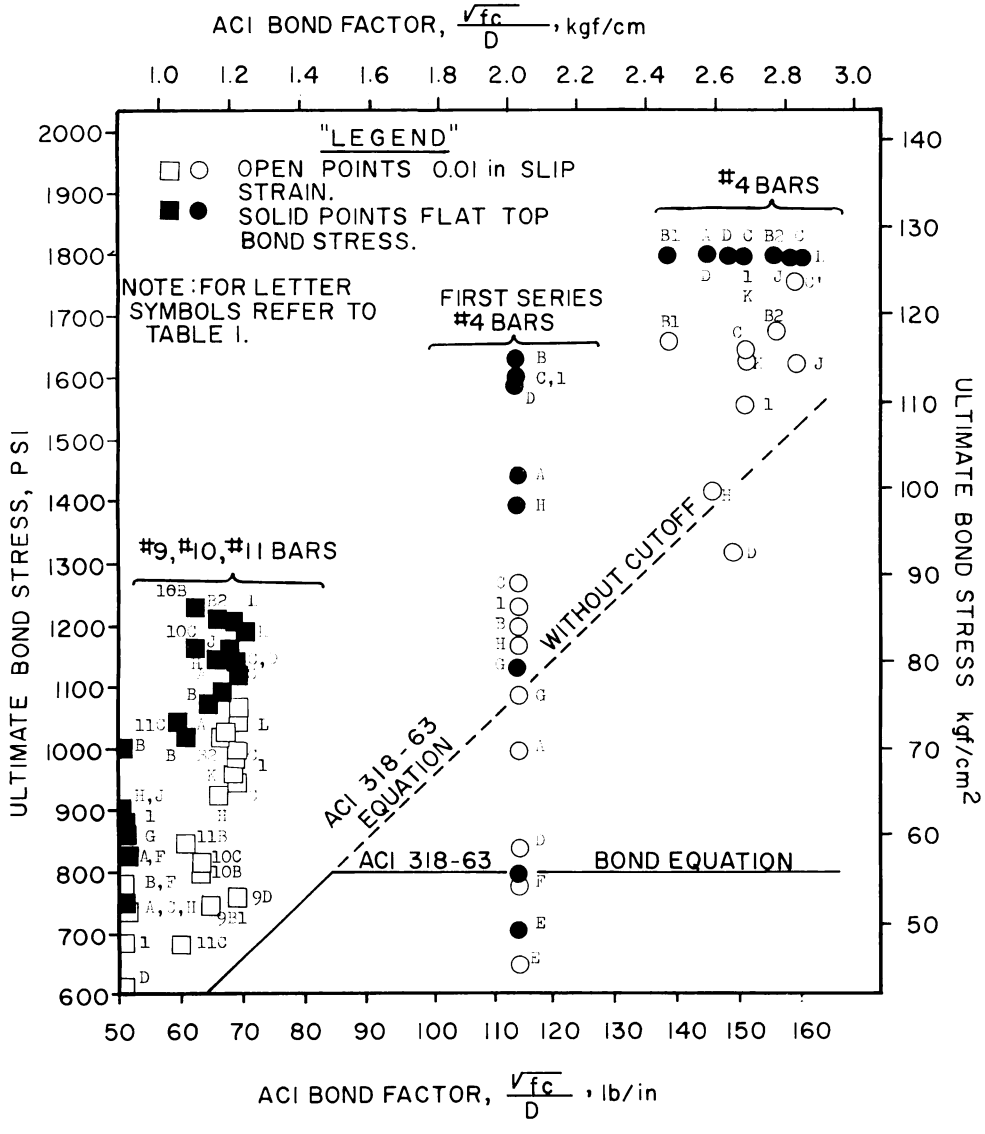

FIGURE 11 - COMPARISON OF TEST DATA WITH ACI BOND REQUIREMENTS.

Fig. 11 — Comparison of test data with ACI bond requirements

TABLE 5 — SELECTED BOND DATA FOR TEST CORRELATION

Type of test	Bar size No.	Cylinder strength f_c', psi (kgf/cm²)	Bond length L_e, in. (cm)	u corresponding to: psi (kgf/cm²)		Bond stress at critical slip psi (kgf/cm²)	Ultimate bond stress psi (kgf/cm²)
				0.01 in. (0.25 mm) Loaded end slip	0.002 in. (0.05 mm) Free end slip		
NBS beam	4	4265 (300)	7 (17.8)	1285 (90.3)	1327 (93.3)	1285 (90.3)	1636 (115.0)
NBS beam	4	4210 (296)	7 (17.8)	1259 (88.5)	1235 (86.8)	1235 (86.8)	1572 (110.5)
NBS pullout	4	4370 (307)	7 (17.8)	760 (53.4)	680 (47.8)	—	1542 (108.4)
NBS pullout	4	4370 (307)	7 (17.8)	790 (55.5)	580 (40.8)	—	1620 (113.9)
Cantilever beam	4	3300 (230)	5 (12.7)	1230 (86.5)	—	1230 (86.5)	1570 (110.4)
NBS beam	8	3585 (252)	14 (35.6)	—	561 (39.4)	561 (39.4)	598 (42.0)
NBS beam	8	4055 (285)	14 (35.6)	710 (49.9)	722 (50.8)	710 (49.9)	760 (53.4)
NBS pullout	8	4300 (302)	14 (35.6)	540 (38.0)	565 (39.7)	—	1371 (96.4)
NBS pullout	8	4300 (302)	14 (35.6)	595 (41.8)	835 (58.7)	—	1394 (98.0)
Cantilever beam	9	3300 (230)	15 (38.1)	780 (54.8)	1000 (70.3)	780 (54.8)	1000 (70.3)

less than half the measured bond capacity of the bars. This is somewhat paradoxical since the smaller bars do not fail by splitting, yet have a more severe allowable ultimate stress limit imposed by the current code.

Instead of using an ultimate stress plotted against $\sqrt{f_c'}/D$, it is also possible to plot the stress which occurs at a loaded end slip of 0.01 in. (0.25 mm), shown as open points in Fig. 11. Comparing the experimental data for this stress level with the ACI bond requirements reveals that this criterion provides an acceptable lower bound for the larger bars, but the 800 psi (56.2 kgf/cm²) maximum is still unrealistically conservative for the smaller bars. If no upper limit were placed on the bond stress, the dotted line on the curve shows that this would form a suitable lower bound on all values except the artificial scale, lubricated, and mechanically clean bars — none of which would be encountered in practice.

By examining the bond-slip curves it can be seen that the concrete strength has much more influence on bond behavior and ultimate bond stress than surface conditions. Comparison of the first and second series shows that increasing concrete strength increases the initial slope of the bond-slip curve, the point of bond breakdown and the ultimate bond stress significantly. Apart from the 800 psi (56.2 kgf/cm²) limit, the ACI bond equation using the $\sqrt{f_c'}/D$ parameter appears to be reasonable (see Fig. 11). This factor is assumed to account for the influence of concrete strength and the ratio of bar perimeter to area. Perhaps a more accurate factor could be determined by regression analysis if there were sufficient data available.

Veracity of new bond test

Since the data obtained were derived from a new type of bond test, it is in order to establish the veracity of this test. Fortunately, previous bond studies by the National Bureau of Standards[7] employed both the hammer head beam and conventional pullout specimens. The results of these tests on "as rolled" bars were compared with similar specimens in the current series. Although bond lengths and concrete strengths were not quite the same, it is evident from Table 5 that the beam test results are in general agreement with the new cantilever test data although neither test data can be correlated with pullout test results.

CONCLUSIONS

On the basis of the experimental research program described above, the important conclusions are as follows:

1. Bond characteristics of deformed (ASTM A305) reinforcing bars of the range of sizes tested would not appear to be adversely affected by varying degrees or types of surface rust or ordinary mill scale, provided the unit weight of a cleaned specimen from the bar meets the minimum ASTM weight and height of deformation requirements. It is not necessary to clean or wipe the bar surface before using it in concrete construction. For any given environment causing rust, the thickness of rust would be about the same regardless of bar size. Therefore, the bond performance relative to rust of larger diameter bars, which have higher deformations, should be superior to that of the bars tested.

2. Comparing the test data for rusted and "as rolled" bars with mill scale indicates that the current bond requirements are quite conservative, especially with regard to the smaller bars because of the 800 psi (56.2 kgf/cm²) maximum stress limit. However, the form of the ACI bond equation using the $\sqrt{f_c'}/D$ factor can be made to correlate satisfactorily with the data.

3. Concrete strength appears to control the overall bond behavior, particularly the amount of slip and deformation, to a much greater extent than the surface condition of the bar.

4. Results obtained with the cantilever test correlate with relatable beam tests. Such specimens are relatively easy to cast and test, while the test itself offers many advantages over the standard pullout test.

ACKNOWLEDGMENTS

The authors wish to acknowledge American Iron and Steel Institute's Committee of Concrete Reinforcing Bar Producers, sponsors of the investigation, and to express appreciation to members of the Committee's Technical Subcommittee for their cooperation and technical assistance.

REFERENCES

1. Withey, M. O., "Tests on Bond Between Concrete and Steel in Reinforced Concrete Beams," *Bulletin* No. 321, University of Wisconsin, 1909.

2. Abrams, Duff A., "Tests of Bond Between Concrete and Steel," *Bulletin* No. 71, University of Illinois, 1913.

3. Shank, J. R., "Effect of Bar Surface Conditions in Reinforced Concrete," *Experiment News*, Ohio State University, V. 6, No. 3, June 1934, pp. 9-12.

4. Gilkey, H. J.; Chamberlin, S. J.; and Beal, R. W., "Bond Tests on Rusted Bars," *Proceedings*, Highway Research Board, V. 19, 1939, pp. 149-163.

5. Johnston, B. G., and Cox, K. C., "The Strength of Rusted Deformed Bars," ACI JOURNAL, *Proceedings* V. 37, 1941, pp. 57-72.

6. USBR, *A Manual for the Control of Concrete Construction*, U.S. Department of the Interior, Bureau of Reclamation (6th edition), 1956.

7. Mathey, R. G., and Watstein, David, "Investigation of Bond in Beam and Pullout Specimens with High Yield Strength Deformed Bars," ACI JOURNAL, *Proceedings* V. 57, No. 9, Mar. 1961, pp. 1071-1090.

8. Clark, Arthur P., "Comparative Bond Efficiency of Deformed Concrete Reinforcing Bars," ACI JOURNAL, *Proceedings* V. 43, No. 4, Dec. 1946, p. 381.

9. Clark, Arthur P., "Bond of Concrete Reinforcing Bars," ACI JOURNAL, *Proceedings* V. 46, No. 3, Nov. 1949, p. 161.

10. ACI Committee 408, "A Guide for Determination of Bond Strength in Beam Specimens," ACI JOURNAL, *Proceedings* V. 61, No. 2, Feb. 1964, pp. 129-136.

11. ACI Committee 318, "Building Code Requirements for Reinforced Concrete (ACI 318-63)," American Concrete Institute, Detroit, 1963, 144 pp.

This paper was received by the Institute Sept. 5, 1967.

Sinopsis—Résumé—Zusammenfassung

Efecto de la Corrosión y las Escamas en las Caracteristicas de Adherencia de Barras de Refuerzo Corrugadas

Se estableció un programa experimental para suministrar información necesaria en las características de adherencia de las barras ASTM A 432 con una amplia variación de escamas y condiciones de corrosión. El parámetro principal en esta serie de ensayes fue la condición superficial de la barra.

Se concluye que las características de adherencia de la barra de refuerzo corrugada con corrugaciones que cumplan con las especificaciones ASTM A 305 no parecen afectarse adversamente por las intensidades variables o tipos de corrosión superficial o escamas producto de la laminación si el peso de la barra cumple con los requisitos mínimos ASTM de peso y de corrugaciones. Las dimensiones de las corrugaciones parecen gobernar las características de adherencia de las barras corroídas; en realidad estas barras presentan un comportamiento similar a barras "laminadas" compañeras. Los datos de ensaye indican que los requisitos actuales de adherencia son bastante conservadores, especialmente en relación a barras más pequeñas debido al límite máximo del esfuerzo de 60 kg/cm^2 (800 lb/pulg^2). La resistencia del concreto parece controlar el comportamiento de la adherencia, particularmente el deslizamiento y las corrugaciones, en un grado mayor que las condiciones superficiales de la barra.

Effets de la Rouille et de l'Ecaillage sur les Caractéristiques d'Adhérence de Barres d'Armature Déformées

Un programme expérimental a été établi pour fournir l'information recherchée sur la caractéristique d'adhérence de barres ASTM A 432 avec éventail très large de conditions de rouille et d'oxydation. Le paramètre principal dans cette série d'essais fut l'état de surface des barres.

Il a été conclu que les caractéristiques d'adhérence de barres d'armature déformées avec des déformations correspondant aux spécifications de l'ASTM A 305 ne semblent pas affectées subséquement par différents degrés aux types de surfaces rouillées ou par un écaillage ordinaire pourvu que le poids de la barre corresponde au poids minimum de l'ASTM et les conditions d'amplitude de déformation. Les dimensions de déformations semblent déterminantes des caractéristiques d'adhérence de barres rouillées; en celà ces barres font apparaitre un comportement similaire à celui de barres "enveloppées". Les résultats d'essais indiquent que les conditions d'adhérence couramment imposées sont tout à fait empiriques, particulièrement pour les petites barres par suite de la contrainte limite maximum de 60 kgf/cm^2 (800 psi). La résistance du béton semble commander le comportement d'adhérence extérieure, en particulier de glissement ou de déformation d'une façon plus certaine que l'état de surface de la barre.

Der Einfluss von Rost und Abplatzungen auf die Verbundeigenschaften von Betonformstählen

Ein Versuchsprogramm wurde aufgestellt, um notwendige Auskünfte über die Verbundeigenschaften von ASTM A 432 Betonstählen zu erarbeiten. Dabei wurden Stähle Der wichtigste Parameter in den Versuchsreihen waren die Oberflächeneigenschaften der Stähle mit verschiedenen Abplatzungs- und Rostgraden untersucht. Aus den Versuchsergebnissen wurde geschlossen, dass die Verbundeigenschaften von Betonformstahlen, die den Vorschriften ASTM A 305 folgen, von Oberflächenrost oder Abplatzungen der Walzhaut nicht negativ beeinflusst werden, solange das Gewicht der Bewehrungsstähle und die Höhe der Rippen den minimalen Anforderungen nach ASTM entsprechen. Die Abmessungen der Rippen kontrollieren die Verbundeigenschaften angerosteter Stähle und verhalten sich ähnlich wie nicht verrostete Vergleichsproben. Die Versuchsergebnisse zeigen, dass die augenblicklichen Anforderungen an den Verbund auf der sicheren Seite liegen; dies ist vor allem der Fall für Stäbe mit kleinerem Durchmesser wegen der auf 800 psi (60 kp/cm^2) beschränkten Maximalspannung. Das allgemeine Verbundverhalten, vor allen Dingen Schlupf und Verformung, scheint von der Betonfestigkeit weit mehr als von der Oberflächenbeschaffenheit der Stäbe abzuhängen.